Article

Method of Extracting the Instantaneous Phases and Frequencies of Respiration from the Signal of a Photoplethysmogram

Ekaterina I. Borovkova [1,2,3], Vladimir I. Ponomarenko [1,4], Anatoly S. Karavaev [1,2,4], Elizaveta S. Dubinkina [1] and Mikhail D. Prokhorov [1,4,*]

[1] Institute of Physics, Saratov State University, 83 Astrakhanskaya St., 410012 Saratov, Russia; rubanei@mail.ru (E.I.B.); ponomarenkovi@gmail.com (V.I.P.); karavaevas@gmail.com (A.S.K.); kometa.ed@gmail.com (E.S.D.)

[2] Institute of Cardiological Research, Saratov State Medical University, 112 Bolshaya Kazachya St., 410012 Saratov, Russia

[3] National Medical Research Center for Therapy and Preventive Medicine, 10 Petroverigsky Per., 101000 Moscow, Russia

[4] Saratov Branch, Institute of Radio Engineering and Electronics, Russian Academy of Sciences, 38 Zelyonaya St., 410019 Saratov, Russia

[*] Correspondence: mdprokhorov@yandex.ru

Abstract: We propose for the first time a method for extracting the instantaneous phases of respiration from the signal of a photoplethysmogram (PPG). In addition to the instantaneous phases of respiration, this method allows for more accurately extracting the instantaneous frequencies of respiration from a PPG than other methods. The proposed method is based on a calculation of the element-wise product of the wavelet spectrum of a PPG and the sequence of intervals between the heartbeats extracted from a PPG, and a calculation of the skeleton of the resulting spectrum in the respiratory frequency range. It is shown that such an element-wise product makes it possible to extract the instantaneous phases and instantaneous frequencies of respiration more accurately than using the wavelet transform of a PPG signal or the sequence of the heartbeat intervals. The proposed method was verified by analyzing the signals from healthy subjects recorded during stress-inducing cognitive tasks. This method can be used in wearable devices for signal processing.

Keywords: instantaneous phases; instantaneous frequencies; photoplethysmogram; electrocardiogram; respiration; RR intervals; wavelet transform; cardiorespiratory interaction; wearable devices

MSC: 37M10

1. Introduction

An interaction of the processes of respiration and autonomic control of blood circulation can be considered an interaction of complex physiological systems, which represent a network of coupled nonlinear oscillators. Therefore, investigations of coherence and synchronization in such complex systems are an important task.

Cardiorespiratory interaction has thus attracted much attention from researchers. Usually, a cardiorespiratory interaction is identified by analyzing the respiratory sinus arrhythmia [1–3] and phase synchronization between the main heart rhythm and respiration [4–9]. However, the interaction between respiration and the low-frequency component of a heart rhythm, which is associated with the process of autonomic control of blood circulation, also plays an important role in the cardiorespiratory interaction. It has been shown that this type of cardiorespiratory interaction is important in studies of sleep [10–12] and healthy aging [13–16], in the assessment of psychophysiological state [17], in the prediction of complications of cardiovascular diseases [18,19], and in basic research [20,21].

Usually, the analysis of a cardiorespiratory interaction is carried out from the analysis of bivariate data, i.e., simultaneously recorded signals of respiration and electrocardiogram

(ECG). However, the cardiorespiratory interaction can be revealed from the analysis of univariate data. In [9], we demonstrated that rhythm, reflecting some properties of the breathing process, can be extracted from the sequence of intervals between the heartbeats. The authors of [9] showed that from the sequence of intervals between the heartbeats, it is possible to extract the main heart rhythm, respiration, and the process of controlling heart rhythm with a frequency of about 0.1 Hz. Then, by determining the instantaneous phases of these rhythms, one can study the cardiorespiratory interaction.

In [22–31], it was reported that the spectral components of the photoplethysmogram (PPG) signal in the high-frequency (HF) range (0.15–0.4 Hz), associated with the frequency of spontaneous respiration of healthy humans, are due primarily to the mechanical contribution of respiration to the dynamics of a PPG. Such results show the promise of using the univariate data of PPG signals for calculating some characteristics of respiration. This is of particular interest in the development of small-sized ergonomic wearable monitoring diagnostic devices [32].

A number of methods have been proposed for extracting the respiratory signal from a PPG signal [33–46]. For example, the respiratory signal can be extracted using bandpass filtering of a PPG with linear filters [33]; discrete wavelet transform [34], including the automatic selection of the mother function for a wavelet transform [35]; a singular spectrum analysis [36]; and a principal component analysis [37] with its modifications: multiscale principal component analysis [38] and modified multi-scale principal component analysis [39].

To increase the accuracy of the estimation of the instantaneous frequency of respiration, methods have been proposed using several surrogate respiratory signals obtained from a univariate PPG [40–43]. In these papers, reference points (systolic and diastolic peaks, etc.) of the PPG were detected and, then, the pulse rate variability, pulse amplitude variability, and pulse width variability were estimated using these reference points. In [40,41], the authors averaged the periodogram pulse rate variability, pulse amplitude variability, and pulse width variability and determined the instantaneous frequency of respiration by analyzing the maximum power of the averaged periodogram in the frequency range of spontaneous breathing. The authors of [42] proposed a method based on a mutual frequency–time analysis of pulse rate variability and pulse amplitude variability. The instantaneous frequency of respiration was determined using the maximum power of the resulting coherence spectrum in the respiratory frequency range. The authors of [43] proposed a method named secondary wavelet feature decoupling to extract the instantaneous frequencies of the respiratory signal.

In [44], the empirical mode decomposition of the PPG signal was used to extract the frequency of respiration. In [45], a neural network was built to extract the periods of inhalation and exhalation from a contactless PPG signal. However, most of the above-mentioned methods demonstrated large errors in the values of instantaneous frequencies of respiration estimated from the PPG signal in comparison with a direct analysis of the respiratory signal. Moreover, there are no studies aimed at extracting the instantaneous phases of respiration from a univariate PPG. The instantaneous phase of the signal is necessary for methods of detecting the phase coherence, phase synchronization, and directed couplings between the elements of multicomponent systems [46]. Thus, the task of extracting the characteristics of a respiratory signal from a univariate PPG signal is an important problem. At the same time, despite a significant number of papers, the accuracy of estimating the instantaneous frequencies of respiration in these studies is worse than when using a direct analysis of the respiratory signal using multichannel data.

Therefore, the goal of this paper is to develop a method of determining the instantaneous phases and instantaneous frequencies of the respiratory signal from the univariate data of a PPG.

2. Materials and Methods

2.1. Design of the Study and the Experimental Data

We analyzed the records of 61 healthy men aged 21 ± 3 years (mean $\pm$ standard deviation) with an average level of physical activity. The study protocol was as follows: 6 min resting period (R1), 6 min of the Stroop color word test (S1), 6 min resting period (R2), and 6 min of the mental arithmetic test (S2). During the experiment, volunteers breathed spontaneously. During stages R1 and R2, volunteers were asked to relax. The protocols for performing the Stroop color word test and mental arithmetic test were taken from [47,48].

During the testing, we recorded the signals of respiration (BR) using a recursion sensor, an ECG in standard Einthoven lead I, and a PPG from the distal phalanx of the left ring finger with a reflected light sensor with a wavelength of 532 nm. All signals were recorded using the standard certified digital electrocardiograph Encefalan_EEGR-19/26 [49] with a 250 Hz sampling frequency and a 16-bit resolution. The signals were filtered at a bandpass of 0.016–70 Hz.

2.2. Methods

We extracted from the ECG signal a sequence of intervals between the heartbeats by detecting the position of R peaks and calculating the time intervals between them (Figure 1a). From the PPG signal, we extracted a sequence of intervals between the heartbeats as the series of intervals between the local positive maximal PPG extremes in consecutive cardiac cycles (Figure 1b). According to the recommendations in [50], nonequidistant sequences of RR intervals and PP intervals were approximated by β-splines and resampled with a frequency of 250 Hz. For brevity, such equidistant realizations obtained from the ECG and PPG were called RR and PP, respectively (Figure 1c). The respiratory signal is shown in Figure 1d.
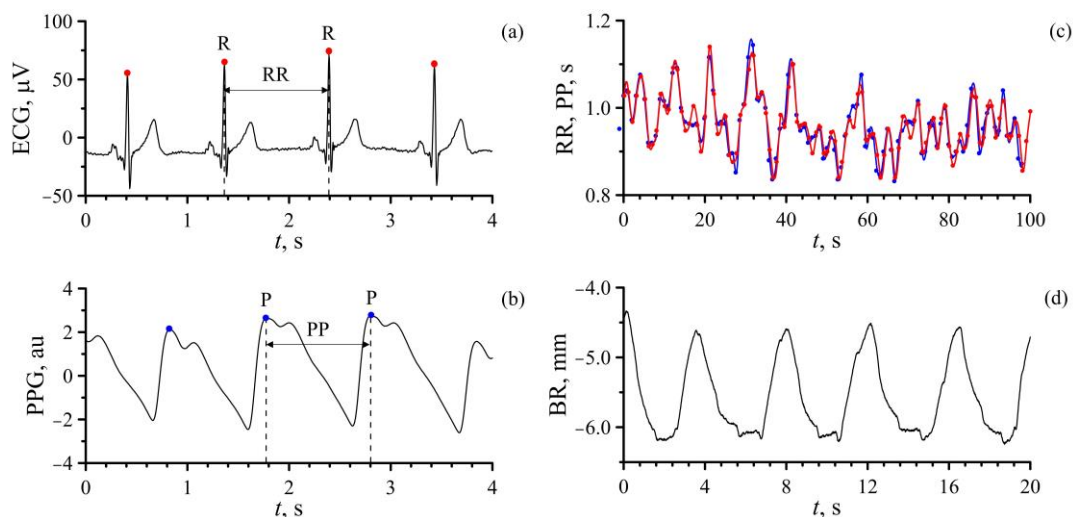
Figure 1. Experimental signals for subject No. 14 at stage R1: (**a**) ECG; (**b**) PPG; (**c**) RR and PP intervals. Nonequidistant sequences of RR and PP intervals are shown with red and blue dots, respectively. Approximations of these sequences are shown with red and blue lines, respectively; (**d**) respiratory signal.

From the RR, PP, and PPG signals, the instantaneous phases and instantaneous frequencies of processes observed at characteristic respiration frequencies of 0.14–0.50 Hz were extracted using wavelet transform [51]. The obtained time series were compared with the realizations of the instantaneous phases and frequencies extracted directly from the time series of the respiratory signal.

We used the continuous wavelet transform of the signal $x(t)$ defined as follows:

$$W(a,b) = \frac{1}{\sqrt{a}} \int_{-\infty}^{\infty} x(t) \psi^*\left(\frac{t-b}{a}\right) dt \qquad (1)$$

where ψ is a basis function; a is the scale variable defining the width of the wavelet; b is the translation variable, which determines the shift in the basis function along the time axis; and a and b are the coefficients of the wavelet transform [51]. As a complex basis function, we chose the Morlet wavelet:

$$\psi(t) = \pi^{-1/4} \exp(jkt) \exp(-t^2/2) \qquad (2)$$

where k is the wavelet parameter, t is a time, and j is the imaginary unit. The choice of wavelet parameter $k = 2\pi$ provided a relationship between the scale parameter and the frequency of the spectral components of the signal f in the form $a = 1/f$, allowing the wavelet spectrum to be expressed in Hz.

In this case, the complex wavelet spectrum can be defined as follows:

$$W(f,b) = |W(f,b)| \exp(-j\Phi(f,b)) \qquad (3)$$

where $|W(f,b)|$ is the amplitude wavelet spectrum (the absolute value of complex function $|W(f,b)|$) and $\Phi(f,b) = \arg W(f,b)$ is the phase wavelet spectrum. The amplitude and phase wavelet spectra of the analyzed signals were used in our paper to extract the instantaneous frequency and phase of the respiratory signal.

To extract the instantaneous frequency of the respiratory signal, the skeletons of these spectra in the respiratory frequency range were calculated using the amplitude wavelet spectra RR, PP, and PPG. To do this, in the specified range for each shift value b, the maximum amplitude $|W(f,b)|$ was determined. The frequency values corresponding to the skeletons of the respiratory signals, RR, PP, and PPG—$f_{\mathrm{BR}}(t)$, $f_{\mathrm{RR}}(t)$, $f_{\mathrm{PP}}(t)$, and $f_{\mathrm{PPG}}(t)$, respectively—were used in the paper as sequences of the instantaneous frequencies of the corresponding signals. The instantaneous phases of the analyzed signals—$\varphi_{\mathrm{BR}}(t)$, $\varphi_{\mathrm{RR}}(t)$, $\varphi_{\mathrm{PP}}(t)$, and $\varphi_{\mathrm{PPG}}(t)$, respectively—were determined from the phase spectrum as phases $\Phi(f,b)$ calculated along the found skeletons.

Breathing is a nonlinear, nonstationary process. The manifestation of its oscillatory activity in the PP and PPG signals is associated with distortions of various natures and interference of components caused by respiratory activity with other processes that have similar frequencies in these signals. We proposed a method aimed at clarifying the position and shape of the instantaneous frequency skeleton in the wavelet spectra of the analyzed PP and PPG signals. The method is based on known data suggesting that the breathing process exhibits oscillatory activity both in the process of heart rate variability and in oscillations of blood supply to the vessels of limbs [22–30]. Moreover, according to these studies, the mechanisms leading to the projection of oscillatory breathing activity onto oscillations in signals associated with heart rate variability and blood pressure fluctuations are fundamentally different [31]. Therefore, we proposed to calculate the element-wise product of the amplitude wavelet spectra of the PP and PPG under the assumption that the frequency components common to these signals associated with respiratory activity will be more contrastingly highlighted against the background of oscillations of a different nature, not associated with the general respiratory signal.

For all time scales f and values of the shift parameter b, the following element-wise product $|W(f,b)|_p$ was calculated as follows:

$$|W(f,b)|_p = (|W(f,b)|_{PP} \odot |W(f,b)|_{PPG})_{f\,b}, \ \forall f, b \qquad (4)$$

where $\odot$ denotes the element-wise product and the brackets mean that we go through all combinations of f and b.

After such an operation, the skeleton $|W(f,b)|_p$ was calculated, similarly to the method described above, as the maximum value of the amplitude spectrum $|W(f,b)|_p$ for each value of the shift parameter b. Using the skeleton, the instantaneous frequency $f_p(t)$ and instantaneous phase $\varphi_p(t)$ of the breathing process were determined. The ratios of instantaneous frequencies $f_{BR}(t)/f_{PP}(t)$, $f_{BR}(t)/f_{PPG}(t)$, and $f_{BR}(t)/f_p(t)$ were calculated and compared with each other.

In addition, for each instantaneous phase difference $\varphi_{BR}(t) - \varphi_{PP}(t)$, $\varphi_{BR}(t) - \varphi_{PPG}(t)$, $\varphi_{BR}(t) - \varphi_p(t)$, $\varphi_{BR}(t) - \varphi_{RR}(t)$, and $\varphi_p(t) - \varphi_{PP}(t)$, the phase coherence coefficient [52] was estimated:

$$\gamma = \sqrt{\langle \cos \Delta\varphi(t) \rangle^2 + \langle \sin \Delta\varphi(t) \rangle^2} \tag{5}$$

where the operator $\langle \rangle$ denotes an average over time and $\Delta\varphi(t)$ is the corresponding difference in the instantaneous phases of oscillations. The obtained values of $\gamma_{BR,PP}$, $\gamma_{BR,PPG}$, $\gamma_{BR,p}$, $\gamma_{BR,RR}$, and $\gamma_{p,PP}$ were compared with each other.

To compare our results from extracting the instantaneous frequencies of respiration from the PPG signal with the results of other authors, we evaluated the root mean squared normalized error (RMSNE) index, defined as follows:

$$\text{RMSNE}_{signal} = \sqrt{\frac{\sum_{i=1}^{n} \left(\frac{f_{BR}(t_i) - f_{signal}(t_i)}{f_{BR}(t_i)} \right)^2}{n}} \cdot 100\% \tag{6}$$

where t_i is the discrete time, n is the number of instantaneous frequency values, $f_{BR}(t_i)$ is the value of the instantaneous frequency of respiration extracted from the wavelet transform skeleton of the respiratory signal, and $f_{signal}(t_i)$ denotes the instantaneous frequency of respiration extracted in another way. "Signal" in (6) can be the PPG, PP, or p.

In addition to a direct comparison of the instantaneous phases and instantaneous frequencies of the analyzed oscillatory processes, their dynamics were studied in the active experiment, in which healthy volunteers completed cognitive tasks. In [17], we showed a statistically significant decrease in coherence between the instantaneous phases of the respiratory signal and RR intervals at stages S1 and S2 in comparison with R1 and R2, respectively. In this paper, we compared the values of the phase coherence coefficient at different stages of the experiments for the instantaneous phases of the analyzed processes, extracted in various ways: from the RR and respiratory signals, as well as from the PP and PPG signals. The median values $\gamma_{BR,RR}^{S1}$, $\gamma_{BR,RR}^{R1}$, $\gamma_{BR,RR}^{S2}$, $\gamma_{BR,RR}^{R2}$, $\gamma_{p,PP}^{S1}$, $\gamma_{p,PP}^{R1}$, $\gamma_{p,PP}^{S2}$, and $\gamma_{p,PP}^{R2}$ calculated at each stage of the experiment and the medians of individual differences $\Delta\gamma_{BR,RR}^{S1} = \gamma_{BR,RR}^{S1} - \gamma_{BR,RR}^{R1}$, $\Delta\gamma_{BR,RR}^{S2} = \gamma_{BR,RR}^{S2} - \gamma_{BR,RR}^{R2}$, $\Delta\gamma_{p,PP}^{S1} = \gamma_{p,PP}^{S1} - \gamma_{p,PP}^{R1}$, and $\Delta\gamma_{p,PP}^{S2} = \gamma_{p,PP}^{S2} - \gamma_{p,PP}^{R2}$ were compared.

We compared the statistical moments of low orders for all indices calculated in our study from experimental signals. During the statistical analysis of the results, the proportion of humans was analyzed for which it was possible to identify a response to cognitive tasks using experimental signals of respiration and RR, or only the univariate signal of PPG.

3. Results

Figure 2 shows the wavelet spectra of the respiratory signal, PP, and PPG, and the element-wise product amplitude wavelet spectra of PP and PPG for subject No.14 at stage R1. These results are typical for all experimental records. The wavelet spectra of signals in Figure 2 make it possible to clearly trace the change over time in the intensity of the oscillation amplitude of the wavelet transform coefficients at different frequency scales.
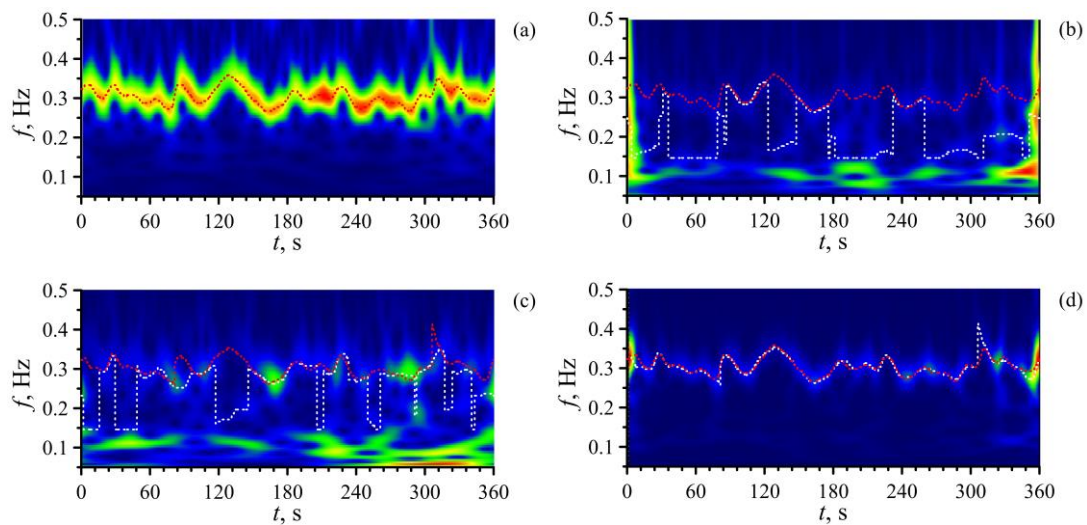
Figure 2. Wavelet spectra of the signals for subject No. 14 at stage R1: (**a**) respiration; (**b**) PP; (**c**) PPG; (**d**) element-wise product of amplitude wavelet spectra of PP and PPG. The color intensity is proportional to the normalized value of the wavelet transform coefficients. The red dotted line marks the skeleton of the respiratory signal. The white dotted line marks the skeleton in the respiratory frequency range of 0.14–0.50 Hz.

The wavelet spectrum of the respiratory signal (Figure 2a) demonstrates clear and contrasting changes over time in the instantaneous frequency of respiration. However, in the spectra of the PP (Figure 2b) and PPG (Figure 2c), the respiratory components, although traceable, are significantly less contrasting. The skeleton of the respiratory signal is shown in Figure 2a–c with a red dotted line. The white dotted line in Figure 2a–c marks the skeleton in the respiratory frequency range of 0.14–0.50 Hz. These figures allow us to trace over time the dynamics of instantaneous frequencies of respiration estimated from various signals. However, a comparison of Figure 2a with Figure 2b,c shows that nonlinear distortions and stochastic influences lead to visually noticeable distortions of the skeletons obtained from the PP and PPG signals with respect to the respiratory signal itself. At the same time, the analysis of the element-wise product and the skeleton calculated from it (Figure 2d) shows, when compared with the wavelet spectrum of respiration (Figure 2a), much better correspondence to the reference respiratory signal.

To compare the capabilities of the wavelet transform in extracting the instantaneous frequencies and instantaneous phases of the breathing process from various signals, we calculated from the skeletons the ratios of instantaneous frequencies of the PP, PPG, and element-wise product to the instantaneous frequency of respiration, as well as the differences between the instantaneous phase $\varphi_{BR}(t)$ and instantaneous phases $\varphi_{PP}(t)$, $\varphi_{PPG}(t)$, and $\varphi_{p}(t)$ (Figure 3).
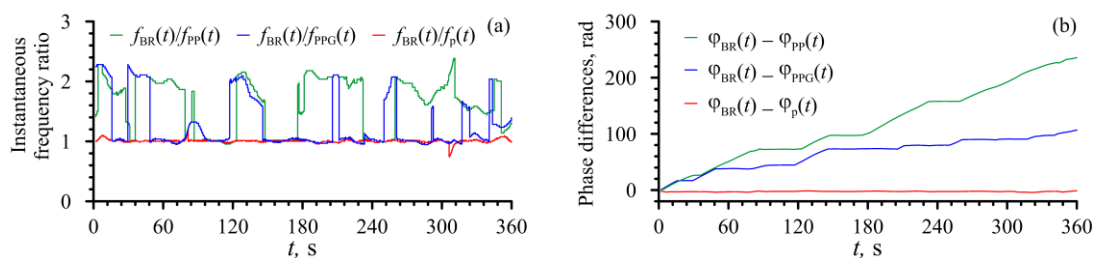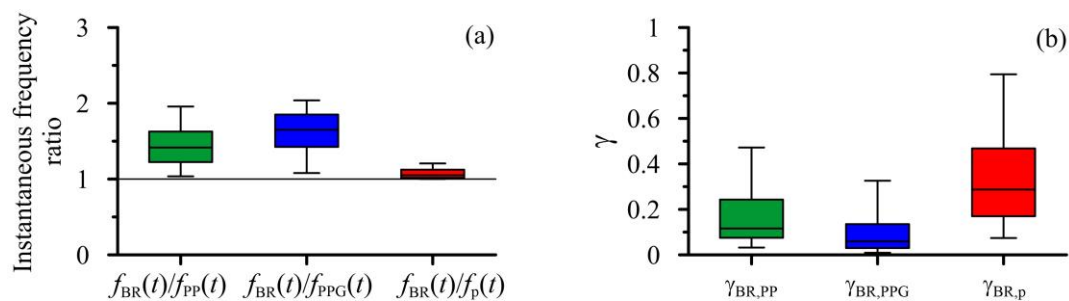

Figure 3. (**a**) Ratios of instantaneous frequencies $f_{BR}(t)/f_{PP}(t)$, $f_{BR}(t)/f_{PPG}(t)$, and $f_{BR}(t)/f_{P}(t)$, and (**b**) instantaneous phase differences $\varphi_{BR}(t) - \varphi_{PP}(t)$, $\varphi_{BR}(t) - \varphi_{PPG}(t)$, and $\varphi_{BR}(t) - \varphi_{p}(t)$ for subject No. 14 at stage R1.

From Figure 3a, it can be seen that the ratio of instantaneous frequencies $f_{BR}(t)/f_p(t)$ remains close to unity throughout the entire record. It indicates a good agreement between $f_{BR}(t)$ and $f_p(t)$. In this case, the ratios $f_{BR}(t)/f_{PP}(t)$ and $f_{BR}(t)/f_{PPG}(t)$ demonstrate large oscillations (Figure 3a). The ratio $f_{BR}(t)/f_{PP}(t)$ turns out to be close to unity only at certain time intervals. The values of $f_{PPG}(t)$ demonstrate slightly better correspondence to $f_{PP}(t)$ than $f_{BR}(t)$ (Figure 3a).

Phase difference $\varphi_{BR}(t) - \varphi_p(t)$ fluctuates around a constant value throughout the entire record (Figure 3b). This behavior of the phase difference indicates a high coherence (the coherence value is 0.86) of the phases $\varphi_{BR}(t)$ and $\varphi_p(t)$, and their closeness. Phase differences $\varphi_{BR}(t) - \varphi_{PP}(t)$ and $\varphi_{BR}(t) - \varphi_{PPG}(t)$ show qualitatively different behaviors (Figure 3b). It can be seen that epochs in which the differences of these phases remain on a flat plateau alternate with epochs of rapid growth of phase differences, corresponding to incoherent behavior. The shortest sections of coherent behavior and rapid increase in the phase difference over time are observed for $\varphi_{BR}(t) - \varphi_{PP}(t)$ (Figure 3b). The coherence between $\varphi_{BR}(t)$ and $\varphi_{PP}(t)$ was 0.09, while the coherence between $\varphi_{BR}(t)$ and $\varphi_{PPG}(t)$ was 0.14.

The results of a quantitative comparison of the capabilities of wavelet spectra in extracting the instantaneous frequencies and instantaneous phases of respiration from PP and PPG at stage R1 are presented in Figure 4 for the entire ensemble of experimental records. Figure 4a shows that the ratio of instantaneous frequencies $f_{BR}(t)/f_p(t)$ for the entire ensemble is significantly closer to 1 (1.05(1.01;1.12), median, first and third quartiles) than $f_{BR}(t)/f_{PP}(t)$ (1.42(1.22;1.62)) and $f_{BR}(t)/f_{PPG}(t)$ (1.65(1.42;1.86)). The last ratio shows the worst correspondence between $f_{PPG}(t)$ and $f_{BR}(t)$ among the compared pairs. An analysis of the phase coherence coefficient (Figure 4b) also confirms the previous conclusions. On average, for the ensemble, the respiratory phase $\varphi_{BR}(t)$ shows the highest coherence with $\varphi_p(t)$ (0.29(0.17;0.47)) and the lowest coherence with $\varphi_{PPG}(t)$ (0.06(0.03;0.14)). The coherence between $\varphi_{BR}(t)$ and $\varphi_{PP}(t)$ was 0.12(0.07;0.24).

Figure 4. Results of a quantitative comparison of the ratios of instantaneous frequencies and phase coherence coefficients for the ensemble of experimental signals at stage R1: (**a**) $f_{BR}(t)/f_{PP}(t)$, $f_{BR}(t)/f_{PPG}(t)$, and $f_{BR}(t)/f_p(t)$. (**b**) $\gamma_{BR,PP}$, $\gamma_{BR,PPG}$, and $\gamma_{BR,p}$. The box boundaries are the first and third quartiles, the horizontal line is the median, and the whiskers are the 5 and 95 percentiles.

To compare our results of extracting the instantaneous frequencies of respiration from the PPG signal with the results of other authors, we calculated the RMSNE measure (6); see Figure 5. This figure shows that the values of $RMSNE_p$ are significantly closer to 0 (1.7(0.7;3.0)) than $RMSNE_{PPG}$ (16.0(10.0;20.7)) and $RMSNE_{PP}$ (11.2(6.3;17.8). Using a direct analysis of the skeleton of the PPG wavelet transform to extract respiration, the authors in [35] estimated the median value of RMSNE as 2.37, which is inferior to our results.
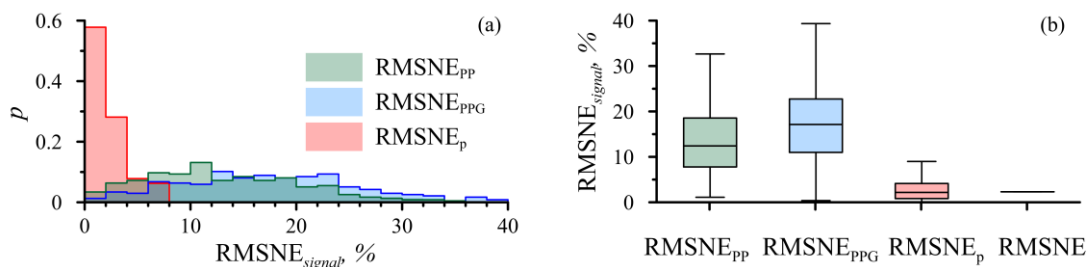
Figure 5. Statistics of the values of RMSNE index at stage R1 for the ensemble of experimental signals: (**a**) histograms of the probability density function of RMSNE$_{signal}$, (**b**) box–whisker diagram for the indicated distributions. The box boundaries are the first and third quartiles, the horizontal line is the median, and the whiskers are the 5 and 95 percentiles. The horizontal line above RMSNE represents the median value obtained for the RMSNE estimation in [35].

Thus, the proposed method of extracting the instantaneous frequencies and phases of respiration from the wavelet spectrum $|W(f,b)|_p$ skeleton made it possible to obtain a noticeably better correspondence to $f_{BR}(t)$ and $\varphi_{BR}(t)$, than when using other methods of extracting the instantaneous frequencies and phases of respiration from PPG.

To assess the possibility of analyzing the instantaneous phases of respiration using a univariate signal of the PPG, the proposed method of $\varphi_p(t)$ extraction was used during the analysis of cardiorespiratory interaction in an active biophysical experiment with a cognitive task. Such physiological tests demonstrated a significant decrease in coherence between $\varphi_{RR}(t)$ and $\varphi_{BR}(t)$ in the majority of subjects during the stages of cognitive task compared to the stages of rest [17].

The experimental signals were analyzed in accordance with the algorithm proposed in [17], with calculations of coherence $\gamma_{BR,RR}$ at all stages of the experiment. From the ensemble of 61 analyzed records, 50 records (82%) were selected that demonstrated a response to cognitive load with a decrease in $\gamma_{BR,RR}$ at least at one of the test stages—S1 or S2—compared with R1 or R2, respectively. For these 50 records, the ability to detect a cognitive load response from a univariate PPG signal using the calculation of $\gamma_{BR,RR}$ and $\gamma_{p,PP}$ was compared.

In accordance with our results obtained in [17], we expect a decrease in the calculated indices at the stages of cognitive load and negative values of individual differences in the indices calculated at the stages of cognitive load and rest. The results of such an analysis and comparison are presented in Figure 6. Figure 6a shows the values of $\gamma_{BR,RR}$, while Figure 6b shows the values of $\gamma_{p,PP}$. It can be seen that both indices demonstrate a pronounced response to cognitive load, decreasing during the transition from R1 to S1 and during the transition from R2 to S2 (Figure 6a,b). An analysis of the statistics of individual differences in coherence coefficients during the transition from rest to cognitive load confirms these conclusions (Figure 6c,d). It can be seen that $\Delta\gamma_{BR,RR}$ (Figure 6c) demonstrates a slightly more pronounced decrease than $\Delta\gamma_{p,PP}$ (Figure 6d). However, the qualitative results of comparing the response to cognitive load for the compared indices are similar.

Among the records of 50 subjects, 35 (70%) subjects showed negative values of index $\Delta\gamma_{BR,RR}^{S1}$ at stage S1, among which 29 (83%) subjects showed negative values of index $\Delta\gamma_{p,PP}^{S1}$. At stage S2, among these 50 subjects, 40 (80%) subjects showed negative values of index $\Delta\gamma_{BR,RR}^{S2}$, among which 28 (70%) subjects showed negative values of index $\Delta\gamma_{p,PP}^{S2}$.
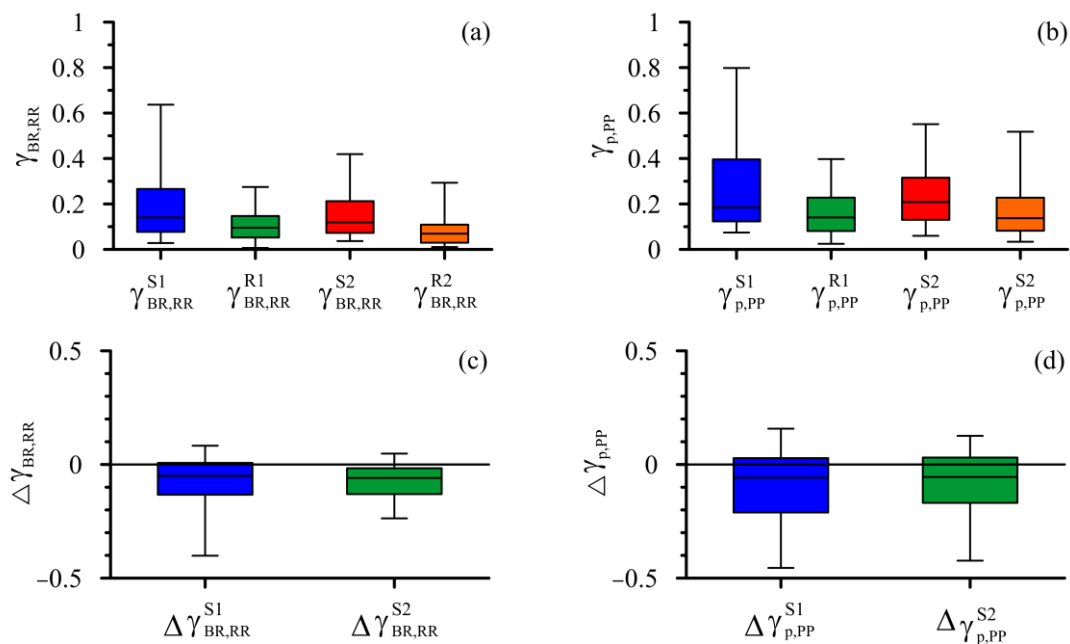
Figure 6. Results of calculating coherence indices from bivariate records of RR and respiration, and univariate record of PPG for an ensemble of 50 volunteers: (**a**) $\gamma_{BR,RR}$ and (**b**) $\gamma_{p,PP}$. Individual differences in coherence indices: (**c**) $\Delta\gamma_{BR,RR}$ and (**d**) $\Delta\gamma_{p,PP}$. The box boundaries are the first and third quartiles, the horizontal line is the median, and the whiskers are the 5 and 95 percentiles.

4. Discussion

We have proposed a new method of determining the instantaneous frequencies and instantaneous phases of the respiratory signal from the PPG signal. The proposed approach increases the accuracy of assessing these characteristics by combining the information about the dynamics of the breathing process extracted from PPG and the sequence of intervals between the heartbeats.

According to a number of studies [22–31], the breathing process manifests itself in PPG as a result of mechanical leakage caused by changes in intrathoracic pressure transmitted along the arterial tree and vasoconstriction of the arteries during inspiration [53] with breathing movements. There is evidence that a decrease in the stroke volume of the heart during inspiration due to changes in intrathoracic pressure, which reduces the amplitude of blood pressure oscillations, also contributes to this process [54].

The mechanisms of manifestation of respiratory activity in the dynamics of the duration of time intervals between the heartbeats are fundamentally different. According to [28,29], there is a complex network of couplings between the structures of the brain stem involved in the regulation of the breathing process and the elements of the parasympathetic and sympathetic branches of the autonomic nervous system, which modulate the heart rate by influencing the pacemakers of the sinoatrial node.

Such qualitatively different mechanisms lead to different nonlinear transformations of the respiratory signal when it is projected into the PPG signal and the sequence of intervals between the heartbeats. In these cases, various stochastic factors act on the path of the respiratory signal. However, information from the sequence of intervals between the heartbeats and from the PPG in the range of respiratory frequencies complements each other, allowing us to extract common components caused specifically by the dynamics of respiration and to weaken the signal components caused by noise and the influence of other processes not related to respiration but with a similar spectral composition: parasympathetic activity, higher harmonics of sympathetic oscillations, etc. The proposed method is based on such reasoning, and in our opinion, the obtained results confirm its promise.

The element-wise product of the amplitudes of the PP and PPG wavelet spectra is the basis of our approach. Such an operation apparently introduces some correlations with these processes into the resulting instantaneous phase.

We believe that this is precisely what accounts for the slight increase in absolute values of $\gamma_{p,PP}$ compared to $\gamma_{BR,RR}$ (Figure 6a,b). At the same time, this artificially introduced coherence practically did not interfere with the detection of various states of subjects in the active experiment (Figure 6c,d). The higher dispersion $\Delta\gamma_{p,PP}$ compared to $\Delta\gamma_{BR,RR}$ is a consequence of a worse signal-to-noise ratio when analyzing the univariate signal of PPG.

Extracting the sequence of intervals between the heartbeats from PPG remains a subject of debate. There are a number of papers that discuss the influence of the modulation of arterial vasomotor tone under the influence of autonomic regulation processes and humoral factors on the signals received from a PPG [26–30]. However, apparently, such influences manifest themselves predominantly in other frequency ranges compared to the respiratory range we are considering, since our comparison of the components of the RR and PP intervals in the analyzed range showed their good quantitative agreement. Minor differences, in our opinion, are due to the greater influence of noise and artifacts on the PPG, which reduce the accuracy of identifying the extremes of this signal compared to the sharply defined R peak of the ECG of healthy subjects. In addition, the analysis of heart rate characteristics based on a single PPG signal, despite the above-mentioned discussion in the literature, is currently widespread, thanks to the wide use of gadgets such as smart watches and fitness bracelets, as well as other wearable devices [55–61]. Hundreds of techniques have been developed to extract the sequence of intervals between the heartbeats from a PPG, including those that work effectively in real time in such wearable devices [62].

We believe that the proposed method for determining the instantaneous phases and instantaneous frequencies of respiration from a univariate signal of PPG may be important for expanding the capabilities of non-invasive ergonomic diagnostics of a human psychophysiological state, primarily using common household wearable devices. In addition, technologies for the contactless registration of PPG using videocameras have recently appeared [63–66].

We used the Morlet wavelet, since it allows one to normalize the scale parameter in Hz. This is convenient for analyzing the values of instantaneous frequencies of respiration. At the same time, the use of another wavelet can potentially increase the accuracy of extracting the characteristics of a respiratory signal from a PPG. The issue of choosing the wavelet mother function was considered in [35] and deserves a separate additional study.

We studied processes with fairly low characteristic frequencies, which were below 0.5 Hz. Therefore, we believe that the sampling rate when implementing the method on wearable devices can be significantly reduced to increase processing speed.

Important issues that we did not consider in our study are the dependence of the obtained results on the PPG sensor placement in other anatomical locations (ear, forehead, forearm, shoulder, wrist, sternum, etc.), the use of sensors with different wavelengths [67], sensor configuration (use of reflected or transmitted light), as well as the impact of motion artifacts on the results, to which the PPG signal is more susceptible than ECG and respiratory signals. We plan to explore these issues in the future.

5. Conclusions

The method of determining the instantaneous phases and instantaneous frequencies of the respiratory signal from the univariate data of a PPG was proposed. This method was based on the element-wise product wavelet spectra of a PPG and the sequence of intervals between the heartbeats extracted from the PPG with the calculation of the skeleton of the resulting spectrum in the respiratory frequency range. The instantaneous phases and instantaneous frequencies of respiration were extracted from the PPG wavelet spectrum along the found skeleton.

It was shown that this element-wise product makes it possible to more accurately identify the instantaneous frequency and instantaneous phase of respiration than can be

achieved using other methods. The ratio of instantaneous frequencies extracted directly from the respiratory signal and using the proposed method was 1.05(1.01;1.12) (median (Q1;Q3)), while the ratio of instantaneous frequencies extracted from the respiratory signal and from PPG was 1.65(1.42;1.86) and the ratio of instantaneous frequencies extracted from the respiratory signal and from the PP intervals was 1.42(1.22;1.62).

A comparison of the proposed method with other methods using the wavelet transform with various mother functions also showed the advantage of our approach. The median value of the RMSNE index was the lowest, equal to 1.7, for our method, while for the methods based on the analysis of the PPG or PP intervals, the median values of the RMSNE index were 16.0 and 11.2, respectively.

In our study, we extracted for the first time the instantaneous phases of a respiratory signal from the univariate signal of a PPG. The proposed method demonstrates high coherence (0.29(0.17;0.47)) of the instantaneous phases extracted directly from the signal of respiration and from the signal of a univariate PPG. In the case of the direct analysis of the PPG and PP intervals, the coherence takes the values 0.06(0.03;0.14) and 0.12(0.07;0.24), respectively.

The proposed method was verified by analyzing the data of healthy subjects in the active experiment while completing cognitive tasks. An analysis of the changes in the values of coherence for the instantaneous phases of the process of controlling the heart rate in the HF band and respiration, extracted from a univariate PPG, showed a decrease in coherence at the stages of the experiment with cognitive loads with respect to the rest stage. For the stage of cognitive load, this change in coherence was $-0.05(-0.13;0.01)$ for the Stroop color word test and $-0.06(-0.13;-0.02)$ for the mental arithmetic test. At the same time, among 50 volunteers for whom such dynamics were identified from the sequence of RR intervals and respiration, the presence of a cognitive load was detected from the univariate PPG signals for 83% of the subjects for the Stroop color word test and 70% of the subjects for the mental arithmetic test. Therefore, the proposed method can be useful for developers of wearable monitoring diagnostic devices.

Author Contributions: Conceptualization, A.S.K. and M.D.P.; formal analysis, E.I.B. and V.I.P.; investigation, E.I.B.; project administration, A.S.K.; software, E.I.B.; supervision, A.S.K.; validation, M.D.P.; visualization, E.S.D.; writing—original draft, E.I.B. and A.S.K.; writing—review and editing, A.S.K. and M.D.P. All authors have read and agreed to the published version of the manuscript.

Institutional Review Board Statement: Not applicable.

Informed Consent Statement: Not applicable.

Data Availability Statement: The datasets are publicly available in the following repository: https://github.com/rubanei/PPG_ECG_Respiration_data (accessed on 31 October 2023).

Conflicts of Interest: The authors declare no conflict of interest.

References

1. Schäfer, C.; Rosenblum, M.G.; Kurths, J.; Abel, H.-H. Heartbeat synchronized with ventilation. *Nature* **1998**, *392*, 239–240. [CrossRef] [PubMed]
2. Angelone, A.; Coulter, N.A. Respiratory sinus arrhythmia: A frequency dependent phenomenon. *J. Appl. Physiol.* **1964**, *19*, 479–482. [CrossRef] [PubMed]
3. Song, H.-S.; Lehrer, P.M. The Effects of Specific Respiratory Rates on Heart Rate and Heart Rate Variability. *Appl. Psychophysiol. Biofeedback* **2003**, *28*, 13–23. [CrossRef] [PubMed]
4. Lotric, M.B.; Stefanovska, A. Synchronization and modulation in the human cardiorespiratory system. *Phys. A Stat. Mech. Its Appl.* **2000**, *283*, 451–461. [CrossRef]
5. Rosenblum, M.G.; Kurths, J.; Pikovsky, A.; Schafer, C.; Tass, P.; Abel, H.-H. Synchronization in noisy systems and cardiorespiratory interaction. *IEEE Eng. Med. Biol. Mag.* **1998**, *17*, 46–53. [CrossRef] [PubMed]
6. Schäfer, C.; Rosenblum, M.G.; Abel, H.-H.; Kurths, J. Synchronization in the human cardiorespiratory system. *Phys. Rev. E* **1999**, *60*, 857–870. [CrossRef] [PubMed]

7. Mrowka, R.; Patzak, A.; Rosenblum, M. Quantitative analysis of cardiorespiratory synchronization in infants. *Int. J. Bifurc. Chaos* **2000**, *10*, 2479–2488. [CrossRef]
8. Prokhorov, M.; Ponomarenko, V.; Gridnev, V.; Bodrov, M.; Bespyatov, A. Synchronization between main rhythmic processes in the human cardiovascular system. *Phys. Rev. E Stat. Nonlin. Soft Matter Phys.* **2003**, *68*, 041913. [CrossRef]
9. Ponomarenko, V.; Prokhorov, M.; Bespyatov, A.; Bodrov, M.; Gridnev, V. Deriving main rhythms of the human cardiovascular system from the heartbeat time series and detecting their synchronization. *Chaos Solitons Fractals* **2005**, *23*, 1429–1438. [CrossRef]
10. Bartsch, R.; Kantelhardt, J.W.; Penzel, T.; Havlin, S. Experimental Evidence for Phase Synchronization Transitions in the Human Cardiorespiratory System. *Phys. Rev. Lett.* **2007**, *98*, 054102. [CrossRef]
11. Borovkova, E.I.; Prokhorov, M.D.; Kiselev, A.R.; Hramkov, A.N.; Mironov, S.A.; Agaltsov, M.V.; Ponomarenko, V.I.; Karavaev, A.S.; Drapkina, O.M.; Penzel, T. Directional couplings between the respiration and parasympathetic control of the heart rate during sleep and wakefulness in healthy subjects at different ages. *Front. Netw. Physiol.* **2022**, *2*, 942700. [CrossRef] [PubMed]
12. Karavaev, A.S.; Skazkina, V.V.; Borovkova, E.I.; Prokhorov, M.D.; Hramkov, A.N.; Ponomarenko, V.I.; Runnova, A.E.; Gridnev, V.I.; Kiselev, A.R.; Kuznetsov, N.V.; et al. Synchronization of the processes of autonomic control of blood circulation in humans is different in the awake state and in sleep stages. *Front. Neurosci.* **2022**, *15*, 791510. [CrossRef] [PubMed]
13. Shiogai, Y.; Stefanovska, A.; McClintock, P.V.E. Nonlinear dynamics of cardiovascular ageing. *Phys. Rep.* **2010**, *488*, 51–110. [CrossRef] [PubMed]
14. Bartsch, R.P.; Schumann, A.Y.; Kantelhardt, J.W.; Penzel, T.; Ivanov, P.C. Phase transitions in physiologic coupling. *Proc. Natl. Acad. Sci. USA* **2012**, *109*, 10181–10186. [CrossRef] [PubMed]
15. Pietri, P.; Stefanadis, C. Cardiovascular Aging and Longevity. *J. Am. Coll. Cardiol.* **2021**, *77*, 189–204. [CrossRef] [PubMed]
16. Ponomarenko, V.I.; Karavaev, A.S.; Borovkova, E.I.; Hramkov, A.N.; Kiselev, A.R.; Prokhorov, M.D.; Penzel, T. Decrease of coherence between the respiration and parasympathetic control of the heart rate with aging. *Chaos* **2021**, *31*, 073105. [CrossRef] [PubMed]
17. Borovkova, E.I.; Hramkov, A.N.; Dubinkina, E.S.; Ponomarenko, V.I.; Bezruchko, B.P.; Ishbulatov, Y.M.; Kurbako, A.V.; Karavaev, A.S.; Prokhorov, M.D. Biomarkers of the psychophysiological state during the cognitive tasks estimated from the signals of the brain, cardiovascular and respiratory systems. *Eur. Phys. J. Spec. Top.* **2023**, *232*, 625–633. [CrossRef]
18. Karavaev, A.S.; Prokhorov, M.D.; Ponomarenko, V.I.; Kiselev, A.R.; Gridnev, V.I.; Ruban, E.I.; Bezruchko, B.P. Synchronization of low-frequency oscillations in the human cardiovascular system. *Chaos* **2009**, *19*, 033112. [CrossRef]
19. Dougherty, C.M.; Burr, R.L. Comparison of heart rate variability in survivors and nonsurvivors of sudden cardiac arrest. *Am. J. Cardiol.* **1992**, *70*, 441–448. [CrossRef]
20. Karavaev, A.S.; Kiselev, A.R.; Runnova, A.E.; Zhuravlev, M.O.; Borovkova, E.I.; Prokhorov, M.D.; Hramov, A.E. Synchronization of infra-slow oscillations of brain potentials with respiration. *Chaos* **2018**, *28*, 081102. [CrossRef]
21. Prokhorov, M.D.; Karavaev, A.S.; Ishbulatov, Y.M.; Ponomarenko, V.I.; Kiselev, A.R.; Kurths, J. Interbeat interval variability versus frequency modulation of heart rate. *Phys. Rev. E* **2021**, *103*, 042404. [CrossRef] [PubMed]
22. Allen, J.; Overbeck, K.; Nath, A.F.; Murray, A.; Stansby, G. A prospective comparison of bilateral photoplethysmography versus the ankle-brachial pressure index for detecting and quantifying lower limb peripheral arterial disease. *J. Vasc. Surg.* **2008**, *47*, 794–802. [CrossRef]
23. Bernardi, L.; Radaelli, A.; Solda, P.L.; Coats, A.J.S.; Reeder, M.; Calciati, A.; Sleight, P. Autonomic Control of Skin Microvessels: Assessment by Power Spectrum of Photoplethysmographic Waves. *Clin. Sci.* **1996**, *90*, 345–355. [CrossRef]
24. FJaved, F.; Middleton, P.M.; Malouf, P.; Chan, G.S.H.; Savkin, A.V.; Lovell, N.H.; Mackie, J. Frequency spectrum analysis of finger photoplethysmographic waveform variability during haemodialysis. *Physiol. Meas.* **2010**, *31*, 1203–1216. [CrossRef]
25. Bernardi, L.; Passino, C.; Spadacini, G.; Valle, F.; Leuzzi, S.; Piepoli, M.; Sleight, P. Arterial Baroreceptors as Determinants of 0.1 Hz and Respiration-Related Changes in Blood Pressure and Heart Rate Spectra. In *Studies in Health Technology and Informatics. Frontiers of Blood Pressure and Heart Rate Analysis*; IOS Press: Amsterdam, The Netherlands, 1997; Volume 35, pp. 241–252. [CrossRef]
26. Ishbulatov, Y.M.; Bibicheva, T.S.; Gridnev, V.I.; Prokhorov, M.D.; Ogneva, M.V.; Kiselev, A.R.; Karavaev, A.S. Contribution of Cardiorespiratory Coupling to the Irregular Dynamics of the Human Cardiovascular System. *Mathematics* **2022**, *10*, 1088. [CrossRef]
27. Dash, S.; Shelley, K.H.; Silverman, D.G.; Chon, K.H. Estimation of Respiratory Rate From ECG, Photoplethysmogram, and Piezoelectric Pulse Transducer Signals: A Comparative Study of Time–Frequency Methods. *IEEE Trans. Biomed. Eng.* **2010**, *57*, 1099–1107. [CrossRef] [PubMed]
28. Guyenet, P.G. Regulation of Breathing and Autonomic Outflows by Chemoreceptors. *Compr. Physiol.* **2014**, *4*, 1511–1562. [CrossRef]
29. Molkov, Y.I.; Zoccal, D.B.; Baekey, D.M.; Abdala, A.P.L.; Machado, B.H.; Dick, T.E.; Rybak, I.A. Physiological and pathophysiological interactions between the respiratory central pattern generator and the sympathetic nervous system. *Breath. Emot. Evol.* **2014**, *212*, 1–23. [CrossRef]
30. Brown, T.E.; Beightol, L.A.; Koh, J.; Eckberg, D.L. Important influence of respiration on human R-R interval power spectra is largely ignored. *J. Appl. Physiol.* **1993**, *75*, 2310–2317. [CrossRef]

31. González, H.; Infante, O.; Lerma, C. Response to active standing of heart beat interval, systolic blood volume and systolic blood pressure: Recurrence plot analysis. In *Translational Recurrences. Springer Proceedings in Mathematics & Statistics*; Springer: Cham, Switzerland, 2014; Volume 103, pp. 109–123. [CrossRef]

32. Charlton, P.H.; Birrenkott, D.A.; Bonnici, T.; Pimentel, M.A.F.; Johnson, A.E.W.; Alastruey, J.; Tarassenko, L.; Watkinson, P.J.; Beale, R.; Clifton, D.A. Breathing Rate Estimation from the Electrocardiogram and Photoplethysmogram: A Review. *IEEE Rev. Biomed. Eng.* **2018**, *11*, 2–20. [CrossRef]

33. Lindberg, L.-G.; Ugnell, H.; Oberg, P. Monitoring of respiratory and heart rates using a fibre-optic sensor. *Med. Biol. Eng. Comput.* **1992**, *30*, 533–537. [CrossRef] [PubMed]

34. Lin, Y.-D.; Chien, Y.-H.; Chen, Y.-S. Wavelet-based embedded algorithm for respiratory rate estimation from PPG signal. *Biomed. Signal Process. Control* **2017**, *36*, 138–145. [CrossRef]

35. Dan, G.; Li, Z.; Ding, H. A Mother Wavelet Selection Algorithm for Respiratory Rate Estimation from Photoplethysmogram. In *World Congress on Medical Physics and Biomedical Engineering*; Jaffray, D., Ed.; Springer: Berlin/Heidelberg, Germany, 2015; Volume 51. [CrossRef]

36. Madhav, K.V.; Krishna, E.H.; Reddy, K.A. Extraction of surrogate respiratory activity from pulse oximeter signals using SSA. In Proceedings of the International Conference on Electrical, Electronics, and Optimization Techniques, Chennai, India, 3–5 March 2016; pp. 1717–1721. [CrossRef]

37. Venu, M.K.; Raghuram, M.; Krishna, E.H.; Reddy, E.; Reddy, K.A. Extraction of respiration rate from ECG and BP signals using order reduced-modified covariance AR technique. In Proceedings of the 2010 3rd International Congress on Image and Signal Processing, CISP, Yantai, China, 16–18 October 2010; Volume 9, pp. 4059–4063. [CrossRef]

38. Venu, M.K.; Raghuram, M.; Krishna, E.H.; Reddy, E.; Reddy, K.A. Use of multi scale PCA for extraction of respiratory activity from photoplethysmographic signals. In Proceedings of the IEEE International Instrumentation and Measurement Technology Conference Proceedings, Graz, Austria, 13–16 May 2012. [CrossRef]

39. Madhav, K.V.; Ram, M.R.; Krishna, E.H.; Komalla, N.R.; Reddy, K.A. Robust Extraction of Respiratory Activity From PPG Signals Using Modified MSPCA. *IEEE Trans. Instrum. Meas.* **2013**, *62*, 1094–1106. [CrossRef]

40. Lázaro, J.; Gil, E.; Bailón, R.; Mincholé, A.; Laguna, P. Deriving Respiration from Photoplethysmographic Pulse Width. *Med. Biol. Eng. Comput.* **2013**, *51*, 233–242. [CrossRef] [PubMed]

41. Karlen, W.; Raman, S.; Ansermino, J.M.; Dumont, G.A. Multiparameter respiratory rate estimation from the photoplethysmogram. *IEEE Trans. Biomed. Eng.* **2013**, *60*, 1946–1953. [CrossRef] [PubMed]

42. Orini, M.; Pelaez-Coca, M.D.; Bailon, R.; Gil, E. Estimation of spontaneous respiratory rate from photoplethysmography by cross time-frequency analysis. *Comput. Cardiol.* **2011**, *38*, 661–664.

43. Addison, P.S.; Watson, J.N. A Wavelet Based Technique to Measure Heart Rate Variability Intern. *J. Wavelets Multiresolut. Inf. Process.* **2004**, *2*, 43–57. [CrossRef]

44. Orphanidou, C. Derivation of respiration rate from ambulatory ECG and PPG using Ensemble Empirical Mode Decomposition: Comparison and fusion. *Comput. Biol. Med.* **2017**, *81*, 45–54. [CrossRef]

45. Johansson, A. Neural network for photoplethysmographic respiratory rate monitoring. *Med. Biol. Eng. Comput.* **2003**, *41*, 242–248. [CrossRef]

46. Kantz, H.; Kurths, J.; Mayer-Kress, G. *Nonlinear Analysis of Physiological Data*; Springer Science & Business Media: Berlin/Heidelberg, Germany, 2012.

47. Stroop, J.R. Near Infrared Spectroscopic Study of Brain Activity during Cognitive Conflicts on Facial Expressions. *J. Exp. Psychol.* **1935**, *18*, 643–662. [CrossRef]

48. Schneider, G.M.; Jacobs, D.W.; Gevirtz, R.N.; O'Connor, D.T.; Hum, J. Cardiovascular haemodynamic response to repeated mental stress in normotensive subjects at genetic risk of hypertension: Evidence of enhanced reactivity, blunted adaptation, and delayed recovery. *J. Hum. Hypertens.* **2003**, *17*, 829–840. [CrossRef]

49. Medicom MTD: Electroencephalographic Studies "Encephalan-EEG". Available online: https://medicom-mtd.com/ (accessed on 23 June 2023).

50. Heart Rate Variability. Standards of Measurement, Physiological Interpretation, and Clinical Use. Task Force of the European Society of Cardiology the North American Society of Pacing Electrophysiology. *Circulation* **1996**, *93*, 1043–1065.

51. Daubechies, I. *Ten Lectures on Wavelets*; Society for Industrial and Applied Mathematics: Philadelphia, PA, USA, 1992.

52. Mormann, F.; Lehnertz, K.; David, P.; Elger, C.E. Mean phase coherence as a measure for phase synchronization and its application to the EEG of epilepsy patients. *Phys. D* **2000**, *144*, 358–369. [CrossRef]

53. Nitzan, M.; Faib, I.; Friedman, H. Respiration-induced changes in tissue blood volume distal to occluded artery, measured by photoplethysmography. *J. Biomed. Opt.* **2006**, *11*, 040506. [CrossRef] [PubMed]

54. Meredith, D.J.; Clifton, D.; Charlton, P.; Brooks, J.; Pugh, C.W.; Tarassenko, L. Photoplethysmographic derivation of respiratory rate: A review of relevant physiology. *J. Med. Eng. Technol.* **2012**, *36*, 1–7. [CrossRef] [PubMed]

55. Nam, Y.; Lee, J.; Chon, K.H. Respiratory Rate Estimation from the Built-in Cameras of Smartphones and Tablets. *Ann. Biomed. Eng.* **2014**, *42*, 885–898. [CrossRef] [PubMed]

56. Karlen, W.; Garde, A.; Myers, D.; Scheffer, C.; Ansermino, J.M.; Dumont, G. A Respiratory rate assessment from photoplethysmographic imaging. In Proceedings of the 36th Annual International Conference of the IEEE Engineering in Medicine and Biology Society, Chicago, IL, USA, 26–30 August 2014; pp. 5397–5400. [CrossRef]

57. Karlen, W.; Garde, A.; Myers, D.; Scheffer, C.; Ansermino, J.M.; Dumont, G. A Estimation of Respiratory Rate From Photoplethysmographic Imaging Videos Compared to Pulse Oximetry. *IEEE J. Biomed. Health Inform.* **2015**, *19*, 1331–1338. [CrossRef]

58. Lázaro, J.; Bailón, R.; Laguna, P.; Nam, Y.; Chon, K.; Gil, E. Respiratory rate influence in the resulting magnitude of pulse photoplethysmogram derived respiration signals. In Proceedings of the Computing in Cardiology, Cambridge, MA, USA, 7–20 September 2014; pp. 289–292.

59. Lázaro, J.; Nam, Y.; Gil, E.; Laguna, P.; Chon, K.H. Respiratory rate derived from smartphone-camera-acquired pulse photoplethysmographic signals. *Physiol. Meas.* **2015**, *36*, 2317–2333. [CrossRef]

60. Yi, W.J.; Park, K.S. Engineering in Medicine and Biology—Derivation of respiration from ECG measured without subject's awareness using wavelet transform. In Proceedings of the IEEE Second Joint EMBS-BMES Conference 2002 24th Annual International Conference of the Engineering in Medicine and Biology Society, Chicago, IL, USA, 30 October–2 November 2002; Volume 1, pp. 130–131. [CrossRef]

61. Alam, R.; Peden, D.; Lach, J. Wearable Respiration Monitoring: Interpretable Inference with Context and Sensor Biomarkers. *IEEE J. Biomed. Health Inform.* **2020**, *25*, 1938–1948. [CrossRef]

62. Mejía-Mejía, E.; May, J.M.; Kyriacou, P.A. Effects of using different algorithms and fiducial points for the detection of interbeat intervals, and different sampling rates on the assessment of pulse rate variability from photoplethysmography. *Comput. Methods Programs Biomed.* **2022**, *218*, 106724. [CrossRef]

63. Sun, Y.; Thakor, N. Photoplethysmography revisited: From contact to noncontact, from point to imaging. *IEEE Trans. Biomed. Eng.* **2016**, *63*, 463–477. [CrossRef] [PubMed]

64. Davis, S.; Watkinson, P.; Guazzi, A.; McCormick, K.; Tarassenko, L.; Jorge, J.; Villarroel, M.; Shenvi, A.; Green, G. Continuous non-contact vital sign monitoring in neonatal intensive care unit. *Healthc. Technol. Lett.* **2014**, *1*, 87–91. [CrossRef]

65. Zaytsev, V.V.; Miridonov, S.V.; Mamontov, O.V.; Kamshilin, A.A. Contactless monitoring of the blood-flow changes in upper limbs. *Biomed. Opt. Express* **2018**, *9*, 5387–5399. [CrossRef] [PubMed]

66. Sagaidachnyi, A.A.; Volkov, I.Y.; Fomin, A.V.; Zaletov, I.S.; Skripal, A.V. A Thermometric Device for Monitoring Oscillations of Peripheral Blood Filling Based on a High-Pass Filter. *Biomed. Eng.* **2012**, *55*, 157–160. [CrossRef]

67. Smolyanskaya, O.A.; Lazareva, E.N.; Nalegaev, S.S.; Petrov, N.V.; Zaytsev, K.I.; Timoshina, P.A.; Tuchin, V.V. Multimodal Optical Diagnostics of Glycated Biological Tissues. *Biochemistry* **2019**, *84*, 124–143. [CrossRef]